

Impedance spectroscopy study of lanthanum-gallium tantalate single crystals grown under different conditions

Ilya M. Anfimov¹, Oleg A. Buzanov², Anna P. Kozlova¹, Nina S. Kozlova¹, Evgeniya V. Zabelina¹

¹ National University of Science and Technology MISiS, 4 Leninsky Prospekt, Moscow 119049, Russia

² SC Fomos-Materials, 16 Buzheninova Str., Moscow 107023, Russia

Corresponding author: Evgeniya V. Zabelina (zabev@mail.ru)

Received 14 January 2019 ♦ Accepted 17 February 2019 ♦ Published 1 June 2019

Citation: Anfimov IM, Buzanov OA, Kozlova AP, Kozlova NS, Zabelina EV (2019) Impedance spectroscopy study of lanthanum-gallium tantalate single crystals grown under different conditions. *Modern Electronic Materials* 5(2): 41–49. <https://doi.org/10.3897/j.moem.5.2.47082>

Abstract

The effect of the growth atmosphere and the type of deposited current conductive coatings on the impedance/admittance of $\text{La}_3\text{Ta}_{0.5}\text{Ga}_{5.5}\text{O}_{14}$ lanthanum-gallium tantalate has been revealed. The lanthanum-gallium tantalate single crystals have been grown in argon and argon with admixture of oxygen gas atmospheres. Current conductive coatings of iridium, gold with a titanium sublayer, and silver with a chromium sublayer have been deposited onto the single crystals. The tests have been carried out taking into account the polarity of the specimens. The temperature and frequency dependences of the admittance of lanthanum-gallium tantalate have been measured in an alternating electric field at frequencies in the 5 Hz to 500 kHz range and temperatures from 20 to 450 °C. The specimens with gold current conductive coating have the lowest admittance. Analysis of the temperature and frequency functions of the dielectric permeability has shown the absence of any frequency dependence in the entire test range.

Equivalent electric circuits have been constructed. Graphic-analytic and numeric analysis of the equivalent electric circuits of the electrode/langatate/electrode cells has shown that the admittance of the metal/langatate/metal cells is controlled by the electrochemical processes at the electrode/electrolyte/electrode interface. The absolute values of the impedance components depend on the langatate growth conditions and the type of the electrodes. Our measurements suggest that the material of the current conductive coating has a greater effect on the absolute values of the measured parameters than the growth atmosphere.

Keywords

langatate, admittance, growth atmosphere, dielectric permeability, impedance spectroscopy

1. Introduction

$\text{La}_3\text{Ga}_{5.5}\text{Ta}_{0.5}\text{O}_{14}$ (LGT) lanthanum-gallium tantalite pertains to the calcium-gallium germanate group crystals of the langasite family which are used in mobile communication system devices, pressure sensors and piezoelectric

sensors of control and monitoring systems based on direct piezoelectric effect. Lanthanum-gallium tantalate finds applications in piezoelectric devices. LGT single crystals have high piezoelectric moduli [1, 2] that are not affec-

ted by temperature drift. This material is distinguished by the absence of phase transitions up to the melting point (1510 °C) [3–5] and the presence of crystallographic orientations with a zero temperature coefficient of elastic oscillation frequency [6, 7].

Lanthanum-gallium tantalate single crystals are grown using the Czochralski method [1, 3, 4]. One of the most serious technological problems is the choice of the growth atmosphere [8–11]. The most common practice of lanthanum-gallium tantalate growth is the use of an argon gas atmosphere with an oxygen addition. The presence of oxygen in the crystal growth atmosphere is required for the prevention of gallium suboxide evaporation which further leads to a deviation from the stoichiometric composition, i.e., gallium evaporation.

Lanthanum-gallium tantalate single crystals grown in different atmospheres differ in color: those grown in an argon atmosphere are almost colorless while those grown in an argon with admixture of oxygen atmosphere have a bright orange color. This is caused by the presence of point defects and their complexes in form of color centers which can be revealed using optical methods, e.g. optical spectroscopy [8, 12, 13].

The application of langatate crystals for the fabrication of high-temperature pressure sensors requires synthesizing these crystals with an electrical conductivity of $\sim 10^{-9} \text{ Ohm}^{-1} \cdot \text{cm}^{-1}$ at $\sim 400 \text{ }^\circ\text{C}$ [1]. The electrical conductivity of langatate crystals is controlled by the presence and concentration of point defects. The growth atmosphere influences the concentration of point defects and hence the carrier concentration. The technology of high-temperature piezoelectric devices uses the polar cuts of the crystals with current conductive coatings deposited.

The polar cut of the $\text{La}_3\text{Ga}_{5.5}\text{Ta}_{0.5}\text{O}_{14}$ crystals, even with symmetrical (similar) electrodes, is an electrochemical cell. The anisotropy of the opposite sides of the crystal polar cuts causes an anisotropy of the near-electrode processes resulting in an acceleration of the overall chemical reactions subject to the possibility of electron passage via an external circuit, i.e., in case of a short circuit. The gradients of the electrochemical potentials and the temperature field in this electrochemical cell produce an EMF and hence short circuit currents. The phenomena of EMF and short circuit currents were first observed and studied in detail in $\alpha\text{-LiIO}_3$ crystals [14, 15]. For other crystals these phenomena were observed and described in [16, 17].

These phenomena have an important practical aspect since the short circuit currents caused by the near-electrode processes may make a substantial contribution to the overall electrical response yielded from the working surface of the piezoelectric sensor. It was reported [18, 19] that the material of the current conductive coatings has a significant effect on the electrophysical parameters of the langatate crystals.

The deposition of current conductive metallic coatings leads to surface degradation due to the electrochemical processes [14] which in turn shortens the service life of the devices, especially at high temperatures.

Therefore studying the electrophysical parameters of the langatate crystals as a function of temperature for different growth conditions, further investigation into the mechanism of interaction between the current conductive coating and the langatate crystal surface and choice of current conductive coating materials are of great practical importance.

2. Materials and methods

The lanthanum-gallium tantalate single crystals were grown and the specimens were prepared by Fomos Materials JSC. The single crystals were Cz grown on Kristall-3M units in iridium crucibles in argon with admixture of oxygen ($\text{Ar} + (2\%) \text{O}_2$) and argon (Ar) gas atmospheres. The crystals were cut into specimens in the form of flat-parallel plates with the working surfaces perpendicular to a 2nd order symmetry axis (polar cuts) and having the thickness $d \sim 1.5 \text{ mm}$ and an area of $\sim 50 \text{ mm}^2$. The specimens were not polarized before the experiments. The following current conductive coatings were deposited onto the specimen surfaces by magnetron sputtering: iridium (Ir), gold (Au), gold with a titanium sublayer (Au(Ti)) and silver with a chromium sublayer (Ag(Cr)).

The specimens were studied in the certified test laboratory Single Crystals and Stock on their Base (National University of Science and Technology MISiS) using certified methods.

The full complex resistance (impedance) of the specimens was measured using the three-electrode method. The temperature and frequency functions of the electrophysical parameters of the specimens in an alternating electric field were measured in the 5 Hz to 500 kHz range on a complex for measuring the electrophysical parameters of high-resistivity crystals the metering unit of which was a Tesla BM 507 impedance meter allowing for impedance measurements from 1 Ohm to 10 MOhm and phase angle measurements from 0 to 90 arc deg. The effective bias voltage was varied automatically from 3 mV to 3 V depending on the measurement range. The frequency dependences were recorded in the 20–450 °C range.

The specimens were placed in a thermal chamber between two symmetrical (made from the same material) clamping electrodes taking into account the polarity of the specimens which was determined using a piezometer under uniaxial compression.

The specimens were heated in the thermal chamber by increasing temperature with 50 °C steps.

The impedance (Z , Ohm) and the phase angle (φ , arc deg) were measured in an alternating electric field. The resultant Z and φ were further used for calculating the total complex conductivity (the admittance, σ) and the relative dielectric permeability (ϵ) using the following formulas:

$$\sigma_z = \frac{d}{S_{el}} \frac{1}{Z} \quad (1)$$

$$\varepsilon = \frac{d}{S_{el}} \frac{1}{2\pi\varepsilon_0} \frac{\sin \varphi}{fZ}, \quad (2)$$

where S_{el} is the electrode area, f is the frequency, Hz, and ε_0 is the dielectric permeability ($\varepsilon_0 = 8.86 \times 10^{-12}$ F/m).

3. Results and discussion

3.1 Impedance spectroscopy

Room temperature impedance spectroscopy measurements showed for all the specimens that their admittance values at 5 Hz in an alternating electric field are 5 orders of magnitude higher than the electrical conductivity in a constant electric field obtained earlier [19] for specimens of the same type. In an alternating electric field with the frequency ranging from 5 Hz to 500 kHz the admittance increased by 3 orders of magnitude in the 20–450 °C range (Figs 1 and 2). The specimens with iridium electrodes cut from the langatate crystal grown in an Ar gas atmosphere do not exhibit any temperature dependence of the admittance up to 350 °C (Fig. 2), with tangible admittance changes starting only at 450 °C with increasing temperature for the entire experimental frequency range. For the crystals grown in an Ar + (2%) O₂ atmosphere, there are no temperature dependence of the admittance in the whole 20–450 °C range (Figs 1 and 2). However, according to the electrical conductivity vs temperature dependence for similar specimens recorded earlier in a constant electric field [19], the electrical conductivity increases by 6–8 orders of magnitude in the same 20–450 °C range.

Study of the temperature and frequency dependences of the admittance for the specimens grown in an Ar + (2%) O₂ atmosphere showed that the specific admittance of the specimens depends on the electrode material (Fig. 1). The lowest admittance was observed for the specimens with gold coatings: their σ_z is by 30 and 20% lower compared with the specimens having silver or iridium electrodes, respectively.

The temperature dependences of the specific admittance for the langatate specimens grown in different atmospheres and having gold and iridium current conductive coatings suggest that the growth atmosphere affects the variation pattern of this parameter (Fig. 2). It should be noted that the effect of the current conductive coating material is greater than that of the growth atmosphere.

Study of the temperature and frequency dependences of the relative dielectric permeability ($\varepsilon_{11}/\varepsilon_0$) for the polar cut specimens with gold, silver and iridium electrodes did not reveal any frequency dependence of the dielectric permeability in the entire experimental frequency range.

The dielectric permeability of the specimens does not depend on temperature up to 400 °C and starts to exhibit temperature dependence at above 450 °C. The relative dielectric permeability was found to depend significantly on the growth atmosphere and the electrode material. Table 1 shows experimental data on the temperature and

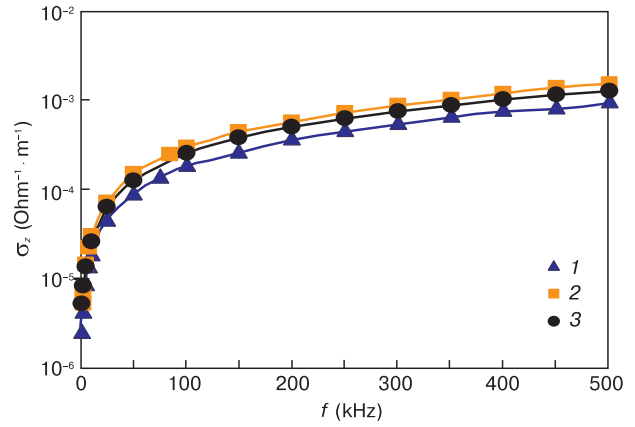


Figure 1. Temperature and frequency dependences of the admittance for the specimens grown in an Ar + (2%) O₂ atmosphere with (1) gold, (2) silver and (3) iridium electrodes.

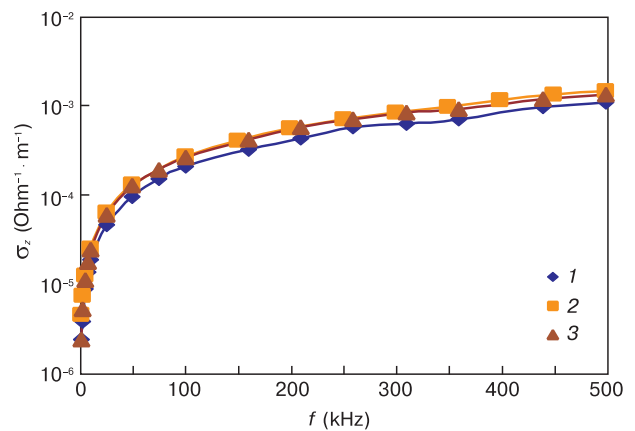


Figure 2. Temperature and frequency dependences of the admittance for the specimens grown in (1, 3) Ar and (2) Ar + (2%) O₂ atmospheres with iridium electrodes: (1) $T = 20, 350$ °C; (2) 20–450 °C; (3) 450 °C.

Table 1. Dielectric permeability ε_{11} at different langatate specimen temperatures in 5 Hz to 500 kHz frequency range.

| Atmosphere | Electrode material | Dielectric permeability | |
|--------------------------|--------------------|-------------------------|------------|
| | | 20–400 °C | 450 °C |
| Ar | Ir | 34 ± 2 | 43 ± 3 |
| Ar + (2 %)O ₂ | Ir | 43 ± 3 | 49 ± 3 |
| Ar + (2 %)O ₂ | Au | 35 ± 2 | 39 ± 3 |

frequency dependences of the relative dielectric permeability for specimens grown in different atmospheres but having similar iridium electrodes. Furthermore, $\varepsilon_{11}/\varepsilon_0$ are shown for specimens grown in the same Ar + (2 %) O₂ atmosphere but having different electrodes. The highest dielectric permeability was observed in the crystals grown in an Ar + (2 %)O₂ atmosphere with iridium current conductive coatings.

Thus the electrode material has a significant effect on the dielectric permeability of the specimens. Our experimental ε_{11} are slightly higher compared with literary data. For example, $\varepsilon_{11} = 26.22$ [20] was obtained at 1 kHz (crystal growth atmosphere N₂ with oxygen addition, cur-

rent conductive coating material not specified) and $\varepsilon_{11} = 19.62$ was obtained at up to 100 kHz (crystal grown by Fomos Materials JSC, growth atmosphere Ar with oxygen addition, current conductive coating Pt/Rh/ZrO₂). This data scatter can be attributed to the differences in the experimental conditions (different frequency ranges), in the crystal growth conditions and in the current conductive coating materials.

Study of the electrophysical properties of langatates showed that the crystals interacted most strongly with gold contacts. X-ray phase analysis of the polar cut surfaces showed that the degradation of the gold coating was the most intense on the surface corresponding to the negative piezoelectric charge. This effect was less pronounced for the specimens with iridium and silver electrodes.

3.2 Construction of equivalent circuits

The most illustrative method of analyzing impedance and admittance measurement results is the construction of a hodograph, i.e., a line in a complex plane described by the free end of the impedance vector with a change in frequency. The shape of the hodograph allows judgment about the equivalent circuit of the process in question and hence about the process itself.

Analysis of the impedance hodographs ($Z'' = f(Z')$) presented in Fig. 3 for the test langatate electrochemical cells grown in different atmospheres and having different current conducting coatings suggests that the properties of these electrochemical cells cannot be described by a trivial equivalent circuit for dielectric crystals which contains parallel-connected double layer capacity C_d and electrolyte bulk resistance R_e .

More complex equivalent circuits are required in order to describe the systems in which the electrodes are at least partially non-blocking. A frequency-controlled diffusion layer forms in the near-electrode space when the system is exposed to alternating current. The oxidation-reduction reactions on the electrode surfaces are caused by the diffusion supply and removal of ions to (from) the solid electrolyte bulk (the langatate crystal). Warburg diffusion impedance emerges in this case

$$(Z_W = (1-j)W_F/\sqrt{\omega}),$$

which includes serial-connected resistance

$$(R_W = W_F/\sqrt{\omega}),$$

where W_F is the Warburg constant and ω is the frequency) and capacity

$$(C_W = 1/(W_F\sqrt{\omega})),$$

which are frequency dependent [22]. We therefore analyzed several equivalent circuits for the electrode / solid electrolyte / electrode system, i.e., the Ershler-Randels and Frumkin-Melik-Gaikazyan ones.

The Ershler-Randels equivalent circuit allows for the presence of electrochemical oxidation-reduction reactions between active ions without specific adsorption of reaction products and charging of the double layer with indifferent ions [21, 22]. The impedance of this reaction can be represented as the impedance of a circuit consisting of serial-connected active resistance R_e describing the charge transfer and Warburg impedance Z_W characterizing the diffusion process. The equivalent circuit has the form presented in Fig. 4.

The Ershler-Randels equivalent circuit is described by the following equation [23, 24]:

$$Z_c = R_e + Z_{el} = R_e + \left(j\omega C_d + \frac{1}{R_F + Z_W} \right)^{-1}, \quad (3)$$

where Z_c is the impedance of the electrode/electrolyte/electrode system (cell), R_e is the active electrolyte resistance, Z_{el} is the impedance of the electrochemical reactions, j is the complex unit, C_d is the capacity of the double layer and R_F is the charge transfer resistance which describes the kinetics of the electrochemical reaction the rate of which is completely controlled by the time of electron attachment or detachment by the electrochemically active particles.

The Ershler-Randels equivalent circuit is not the only possible method of describing the processes taking place in solid electrolyte electrochemical cells. This circuit does not take into account the specific adsorption of the electrochemical reaction products. The problem of impedance with allowance for the adsorption processes was first solved by the authors of an earlier work [23]. It should be noted that in another work referred to above [18], X-ray phase analysis was used for the characterization of the phase composition of the specimen surfaces, e.g. the formation of new different phases on the opposite surfaces of the polar cuts which partially results from the adsorption processes occurring in the near-electrode layers of the specimens with electrodes and making the principal contribution to the resistance of metal/langatate/metal structures. This makes it reasonable to consider the Frumkin-Melik-Gaikazyan equivalent circuit [24, 25]. This circuit is shown in Fig. 5 and describes the electrochemical reactions with allowance for the adsorption of the electrochemical reaction products in electrode / solid electrolyte / electrode systems. The impedance for this circuit is described as follows:

$$Z_c = R_e + \left(j\omega C_d + \frac{1}{R' + Z_W + 1/(j\omega C')} \right)^{-1}, \quad (4)$$

where R' is the resistance characterizing the proper time of the elementary adsorption/desorption cycle, C' is the additional capacity of the double layer associated with the adsorption of the surfactant particles and C_d is part of the double layer capacity caused by indifferent ions.

Based on the experimental results obtained by impedance spectroscopy we determined the components of the complex resistance Z for the abovementioned equivalent circuits

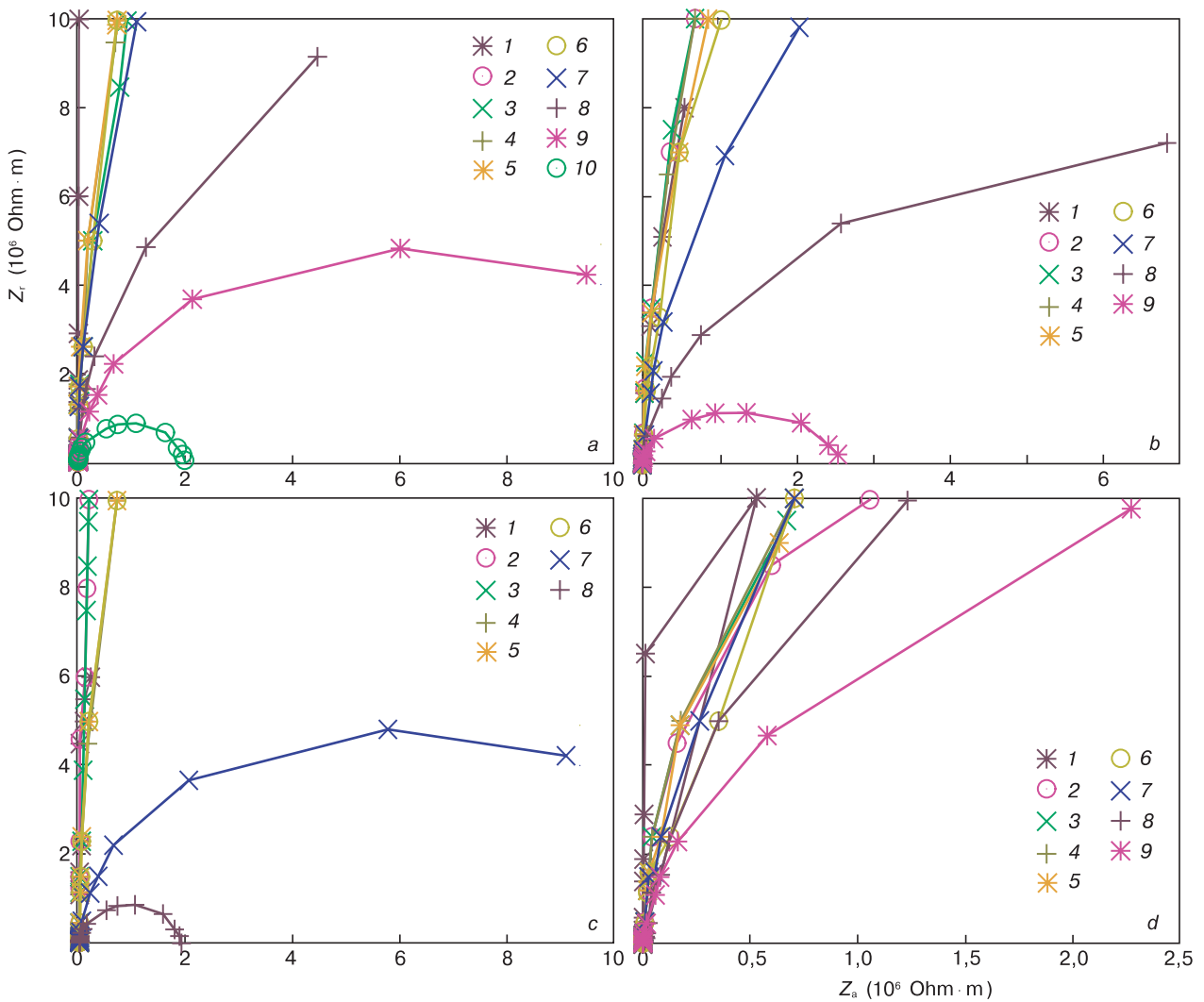


Figure 3. Impedance hodographs for the test langatate electrochemical cells grown in different atmospheres and having different current conducting coatings: (a) Ar + (2%) O₂, Au ((I) T = 20 °C; (2) 50; (3) 100; (4) 150; (5) 200; (6) 250; (7) 300; (8) 350; (9) 400; (10) 450); (b) Ar + O₂, Ir ((I) T = 20 °C; (2) 100; (3) 150; (4) 200; (5) 250; (6) 300; (7) 350; (8) 400; (9) 450); (c) Ar, Au(Ti) ((I) T = 20 °C; (2) 50; (3) 100; (4) 150; (5) 200; (6) 230; (7) 400; (8) 450); (d) Ar, Ir ((I) T = 20 °C; (2) 50; (3) 100; (4) 150; (5) 200; (6) 250; (7) 300; (8) 350; (9) 400).

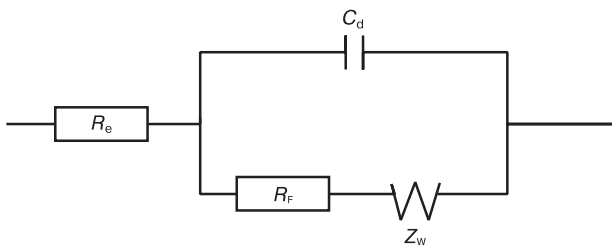


Figure 4. Ershler-Randels equivalent circuit [24, 25].

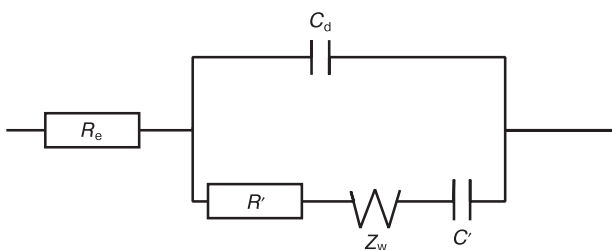


Figure 5. Frumkin-Melik-Gaikazyan equivalent circuit [24, 25].

for all the specimens using an analytical method. The basic principle of the analytical method used is the construction of sets of equations (5)–(12) to include the experimentally measured parameters (ω , $|Z|$ and φ) and coefficients composed of the electrochemical impedance components [24].

For analysis of the Ershler-Randels equivalent circuit and the equation describing this circuit we will introduce the following notations [24]:

$$\frac{1}{j\omega} = x^2 \tag{5}$$

Then

$$x = \frac{1-j}{\sqrt{2}} \omega^{-0.5}; x^2 = -j\omega^{-1}; x^3 = -\frac{1+j}{\sqrt{2}} \omega^{-1.5};$$

$$x^4 = -\omega^{-2}; x^5 = -\frac{1-j}{\sqrt{2}} \omega^{-2.5};$$

Equation (4) can be rewritten as follows [24]:

$$Z_c = \frac{\sqrt{2}a_3x^3 + a_2x^2 + \sqrt{2}a_1x + a_0}{b_2x^2 + \sqrt{2}b_1x + b_0}, \quad (6)$$

where $a_0 = R_e R_F C_d$; $a_1 = R_e W_F C_d$; $a_2 = R_F + R_e$; $a_3 = W_F$; $b_0 = R_F C_d$; $b_1 = W_F C_d$; $b_2 = 1$.

Alternatively, the impedance of the cell can be written in the following form [24, 25]:

$$Z_c = Z_a - jZ_r, \quad (7)$$

where $Z_a = Z \sin\phi$ and $Z_r = Z \cos\phi$.

Substituting the result into Eq. (6) and equalizing the real and imaginary components we obtain two equations with six variables [24]:

$$a_0 + a_1\omega^{-0.5} - a_3\omega^{-1.5} - b_1(Z_a - Z_r)\omega^{-0.5} - b_0Z_a = Z_r\omega^{-1} \quad (8)$$

$$a_1\omega^{-0.5} + a_2\omega^{-1} + a_3\omega^{-1.5} - b_1(Z_a + Z_r)\omega^{-0.5} - b_0Z_r = Z_a\omega^{-1}. \quad (9)$$

We take three frequency values and the respective Z_a and Z_r and as a result obtain a system of six linear equations with six variables a_0 , a_1 , a_2 , a_3 , b_0 and b_1 . Solving the set of equations we obtain the parameters of the equivalent circuit from the following equations:

$$R_e = \frac{a_0}{b_0}; \quad C_d = \left[\left(\frac{a_2}{b_0} \right) - \left(\frac{R_e}{b_0} \right) \right]^{-1}; \quad RC_d = (\omega C_d)^{-1};$$

$$R_F = a_2 - R_e; \quad W_F = a_3; \quad C_w = (W_F \sqrt{\omega})^{-1}; \quad R_w = \frac{W_F}{\sqrt{\omega}}$$

For the Frumkin-Melik-Gaikazyan equivalent circuit the full impedance of the system is written as follows [24]:

$$Z_c = \frac{a_4x^4 + \sqrt{2}a_3x^3 + a_2x^2 + \sqrt{2}a_1x + a_0}{b_2x^2 + b_1x\sqrt{2} + b_0}, \quad (10)$$

where

$$a_0 = \frac{R' R_e C_d}{1 + C_d (C')^{-1}}; \quad a_1 = \frac{W R_e C_d}{1 + C_d (C')^{-1}}; \quad a_2 = R_e + \frac{R'}{1 + C_d (C')^{-1}};$$

$$a_3 = \frac{W}{1 + C_d (C')^{-1}}; \quad a_4 = \frac{(C')^{-1}}{1 + C_d (C')^{-1}};$$

$$b_0 = \frac{R' C_d}{1 + C_d (C')^{-1}}; \quad b_1 = \frac{W C_d}{1 + C_d (C')^{-1}}; \quad b_2 = 1;$$

Separating the terms with real and imaginary coefficients we obtain two linear equations with seven variables [24]:

$$a_0 + a_1\omega^{-0.5} - a_3\omega^{-1.5} - a_4\omega^{-2} - b_1(Z_a + Z_r)\omega^{-0.5} - b_0Z_a = -Z_r\omega^{-1}; \quad (11)$$

$$a_1\omega^{-0.5} + a_2\omega^{-1} + a_3\omega^{-1.5} - b_1(Z_a + Z_r)\omega^{-0.5} - b_0Z_r = Z_a\omega^{-1}. \quad (12)$$

The coefficients a_i and b_i can be found by constructing a set of eight equations with seven variables. Solution of that set of equations allows determining the parameters of the equivalent circuit from the following equations [24]:

$$R_e = \frac{a_0}{b_0}; \quad C_d = \left[\left(\frac{a_2}{b_0} \right) - \left(\frac{R_e}{b_0} \right) \right]^{-1}$$

$$R_{cd} = (\omega C_d)^{-1}; \quad R' = b_0 \left[(C')^{-1} + (C_d)^{-1} \right]$$

$$C' = a_4^{-1} - C_d; \quad R_{c'} = (\omega C')^{-1}$$

$$W_F = \frac{R' b_1}{b_0}; \quad C_w = (W_F \sqrt{\omega})^{-1}; \quad R_w = \frac{W_F}{\sqrt{\omega}}$$

By way of example we present the results of Z component calculation using the Ershler-Randels equivalent circuit (Table 2) and the Frumkin-Melik-Gaikazyan equivalent circuit (Table 3) for the Au/langatate/Au electrochemical circuit (growth atmosphere Ar + (2 %) O₂).

The effect of the impedance components in the equivalent circuits is determined by analyzing the experimental results using three criteria:

– if $R_{cd} \gg R^*$, then $Z_c = R_e + R^*$,

where $R^* = R_F + R_w$ for the Ershler-Randels equivalent circuit or $R^* = R' + R_w + R_{c'}$ for the Frumkin-Melik-Gaikazyan equivalent circuit;

– if $R_{cd} \ll R^*$, then $Z_c = R_e + R_{cd}$;

– if $R_{cd} \approx R^*$, then $Z_c = R_e + (R_{cd} R^* / (R_{cd} + R^*))$.

Analysis of the impedance components showed that the impedance of the electrochemical cells considered is mainly controlled by the processes occurring in the near-electrode regions. At room temperature the resistance of the electrolyte itself R_e is by 2–4 orders of magnitude lower than the resistance of the near-electrode regions (R_{cd} , R' , R_w and $R_{c'}$). It is only at high frequencies (about 500 kHz) and temperatures (above 450 °C) that the resistances of the near-electrode reactions and the electrolyte R_e become comparable and the properties of the electrolyte itself start to show. A similar impedance dependence is observed in the Au/langatate/Au solid electrolyte cells (growth atmosphere Ar) and the Ir/langatate/Ir solid electrolyte cells (growth atmosphere Ar + (2 %) O₂).

At room temperature the impedance of the Ag/langatate/Ag and Ir/langatate/Ir cells (growth atmosphere Ar + (2 %) O₂) depends most significantly on the resistance of the double layer. Whereas for the Ershler-Randels equivalent circuit the difference between the double lay-

Table 2. Parameters of the Ershler-Randels equivalent circuit for the Au/langatate/Au electrochemical circuit (growth atmosphere Ar + (2 %) O₂).

| ω Hz | $Z_c, 10^5 \text{ Ohm}$ | | $R_s, 10^3$ Ohm \times m | $C_d, 10^{-10}$ F/m ² | $R_{cd}, 10^5$ Ohm \times m | $R_f, 10^6$ Ohm \times m | $W_f, 10^{18}$ Ohm \times m \times s ^{-1/2} | $R_w,$ Ohm \times m | $C_w,$ F/m ² |
|----------------|-------------------------|------------|-------------------------------|-------------------------------------|----------------------------------|-------------------------------|---|--------------------------|----------------------------|
| | Experimental | Calculated | | | | | | | |
| At 20 °C | | | | | | | | | |
| 2500 | 60 | 60 | 1 | 0.7 | 60 | 70 | 50 | 1×10^8 | 4×10^{-12} |
| 100 000 | 1 | 1 | | | 1 | | | 2×10^7 | 6×10^{-13} |
| 500 000 | 0.3 | 0.3 | | | 0.3 | | | 8×10^6 | 3×10^{-13} |
| At 450 °C | | | | | | | | | |
| 2500 | 20 | 20 | 2 | 1 | 40 | 3 | 0.4 | 8×10^5 | 5×10^{-10} |
| 100 000 | 1 | 1 | | | 1 | | | 1×10^5 | 8×10^{-11} |
| 500 000 | 0.2 | 0.2 | | | 0.2 | | | 5×10^4 | 4×10^{-11} |

Table 3. Parameters of the Frumkin-Melik-Gaikazyan equivalent circuit for the Au/langatate/Au electrochemical circuit (growth atmosphere Ar + (2 %) O₂).

| ω Hz | $Z_c, 10^5 \text{ Ohm}$ | | $R_s, 10^3$ Ohm \times m | $C_d, 10^{-10}$ F/m ² | $R_{cd}, 10^5$ Ohm \times m | $R_f, 10^6$ Ohm \times m | $W_f, 10^{18}$ Ohm \times m \times s ^{-1/2} | $R_w,$ Ohm \times m | $C_w,$ F/m ² |
|----------------|-------------------------|------------|-------------------------------|-------------------------------------|----------------------------------|-------------------------------|---|--------------------------|----------------------------|
| | Experimental | Calculated | | | | | | | |
| At 20 °C | | | | | | | | | |
| 2500 | 60 | 60 | 3 | 6 | 6×10^6 | 50 | 1×10^8 | 30 | 10 |
| 100 000 | 1 | 2 | | | 2×10^5 | | 3×10^6 | 5 | 2 |
| 250 000 | 0.5 | 0.7 | | | 6×10^4 | | 1×10^6 | 3 | 1 |
| 500 000 | 0.3 | 0.3 | | | 3×10^4 | | 6×10^5 | 2 | 1 |
| At 450 °C | | | | | | | | | |
| 2500 | 20 | 50 | 50 | 3 | 1×10^7 | 0.4 | 9×10^5 | 4 | 90 |
| 100 000 | 1 | 7 | | | 3×10^5 | | 2×10^4 | 0.7 | 10 |
| 250 000 | 0.5 | 3 | | | 1×10^5 | | 9×10^3 | 0.4 | 9 |
| 500 000 | 0.2 | 1 | | | 7×10^4 | | 5×10^3 | 0.3 | 6 |

er resistance R_{cd} and the impedance caused by the electrochemical reactions ($R_f + R_w$) is 1–2 orders of magnitude, for the Frumkin-Melik-Gaikazyan equivalent circuit the difference between R_{cd} and ($R_f + R_w + R_c$) is 2–3 orders of magnitude. Another impedance dependence is observed for the Ir/langatate/Ir cells (growth atmosphere Ar): at room temperature Z_c for the Frumkin-Melik-Gaikazyan equivalent circuit is controlled by the adsorption/desorption electrochemical processes (R_f, R_w and R_c), while for the Ershler-Randels equivalent circuit Z_c is controlled by R_{cd} ; with an increase in temperature (same as for the Ag/langatate/Ag cell (growth atmosphere Ar + (2 %) O₂)) the double layer charging resistance makes the largest contribution.

These results suggest that the impedance of the Ir/langatate/Ir, Au/langatate/Au (growth atmosphere Ar + (2 %) O₂) and the Au/langatate/Au (growth atmosphere Ar) cells is largely controlled by the double layer resistance (at temperatures of about 20 °C) and the resistance caused by the electrochemical reactions at the electrode/electrolyte/electrode interface (at high temperatures). On the contrary, the impedance of the Ag/langatate/Ag cell (growth atmosphere Ar + (2 %) O₂) and the Ir/langatate/Ir (langatate growth atmosphere Ar) cell is controlled by the double layer resistance in the entire experimental temperature range. The highest resistance R_w was observed for the Ir/langatate/Ir cell and the lowest one, for the Au/langatate/Au cell. Thus, there is a clear dependence of the impedance/admittance of the metal/langatate/metal systems both on the material of the current

conductive coating and on the measurement temperature and frequency.

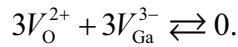
Analysis of our calculation results does not suggest definitively that preference should be given to either of the two equivalent circuits since the contribution of the observed adsorption processes to the impedance of the cells is very small.

It is assumed that langatate contains two types of ions:

- indifferent carriers which participate in the charge transfer via the electrolyte and control its bulk resistance but do not take part in the electrochemical reactions occurring at the electrode/electrolyte boundary;
- active ions which participate in the electrochemical reactions.

In accordance with the earlier reported defect formation model for langatate crystals [12, 13], the main types of defects in these crystals are oxygen and gallium vacancies and their complexes. Studies of the electrophysical properties of the crystals [18, 19], e.g. the phenomenon of current degradation in time, suggest the predominant ionic mechanism of the electrical conductivity which is in a good agreement with earlier literary data [26, 27]. Although different langatate crystal electrical conductivity models are currently available, the authors of all the referred works have concluded that the low-temperature electrical conductivity occurs predominantly by impurities or electrons whereas the high-temperature electrical conductivity is predominantly ionic.

Thus, oxygen and gallium vacancies are indifferent carriers which participate in the charge transfer via the solid electrolyte and control its bulk resistance. In this case the basic electrical neutrality equation is written in the following form:



When an electric field is applied the oxygen vacancies rush toward the negatively charged electrode (cathode) resulting in an excess of oxygen ions at the positive electrode (anode), whereas gallium vacancies rush toward the anode causing an excess of gallium ions at the cathode. It seems that the oxygen and gallium ions are those active particles which participate in the near-electrode electrochemical reactions.

Expectably, at least one form of electrochemically active matter (oxygen or gallium ions) or both of them enter into reaction and are adsorbed at the electrode in the form of electrochemical reaction products. Since the same particles participate in the Faraday process and in the double layer charging, one cannot clearly distinguish between the charging current and the Faraday current. These processes end up interrelated, and one can in fact judge about a single electrochemical process which results in the change of the electrode surface state and in the occurrence of the oxidation-reduction reactions.

The model suggested here is based on the assumption that the charging of the double electric layer, i.e., the accumulation or deficiency of indifferent ions at the electrode/electrolyte interface, should be accompanied by redistribution of electrochemically active ions. If this is true, this redistribution will show itself in the impedance

measurements as a relaxation process of charging the capacitance C' via the active resistance R' and the diffusion impedance Z_w .

4. Conclusion

The effect of the growth atmosphere and the type of deposited current conductive coatings on the impedance/admittance of lanthanum-gallium tantalate was revealed. The admittance of the specimens with gold coating is 30% lower than that of the specimens with gold electrodes and 20% lower than that of the specimens with iridium electrodes. We show that the specific admittance of the test langatate crystals does not depend on temperature if the impedance is measured in an alternating electric field at temperatures below 400 °C. The langatate growth atmosphere was shown to influence the specific dielectric permeability (ϵ_{11}/ϵ_0) of the polar cuts of the langatate crystals. The dielectric permeability ϵ_{11} proved to be temperature dependent in the entire experimental frequency range.

Information on the origins of the impedance components for langatate with deposited electrodes was obtained by analyzing equivalent circuits for the electrode/langatate/electrode cells using graphic-analytic and numeric methods.

Construction of equivalent circuits and analysis of the hodographs and calculated impedance components showed that the admittance of the metal/langatate/metal cells is controlled by the electrochemical processes at the electrode/electrolyte/electrode interface. The impedance components depend on the growth atmosphere, the electrode material and the measurement temperature and frequency.

References

1. Takeda H., Tanaka S., Izukawa S., Shimizu H., Nishida T., Shiosaki T. Effective substitution of aluminum for gallium in langasite-type crystals for a pressure sensor use at high temperature. *Proc. IEEE Ultrasonics Symp.* 2005; 1(18–21): 560–563. <https://doi.org/10.1109/ULTSYM.2005.1602915>
2. Fukuda T., Takeda H., Kawanaka H., Shimamura K., Kumatoriya M., Murakami S., Sato J., Sato M. Growth of new langasite single crystal for piezoelectric application. *Proc. IEEE Frequency Control Symp.* 1998: 315–319. <https://doi.org/10.1109/ISAF.1998.786697>
3. Shimamura K., Takeda H., Kohno T., Fukuda T. Growth and characterization of lanthanum gallium silicate $\text{La}_3\text{Ga}_5\text{SiO}_{14}$ single crystals for piezoelectric applications. *J. Cryst. Growth.* 1996; 163(4): 388–392. [https://doi.org/10.1016/0022-0248\(95\)01002-5](https://doi.org/10.1016/0022-0248(95)01002-5)
4. Grinev B.V., Dubovik M.F., Tolmachev A.V. *Opticheskie monokristally slozhnykh oksidnykh soedinenii* [Optical single crystals of complex oxide compounds]. Kharkov: Institut monokristallov, 2002. 280 p. (In Russ.)
5. Bohm J., Heimann R.B., Hengst M., Roewer R., Schindler J. Czochralski growth and characterization of piezoelectric single crystals with langasite structure: $\text{La}_3\text{Ga}_5\text{SiO}_{14}$ (LGS), $\text{La}_3\text{Ga}_5\text{Nb}_5\text{O}_{14}$ (LGN) and $\text{La}_3\text{Ga}_5\text{Ta}_5\text{O}_{14}$ (LGT): Pt I. *J. Cryst. Growth.* 1999; 204(1–2): 128–136. [https://doi.org/10.1016/S0022-0248\(99\)00186-4](https://doi.org/10.1016/S0022-0248(99)00186-4)
6. Andreev I.A. Langasite family single crystals – an unusual combination of properties for applications in acoustoelectronics. *Zhurnal tekhnicheskoi fiziki = Technical Physics.* 2006; 76(6): 80–86. (In Russ.)
7. Grouzinenko V.B., Bezdelkin V.V. Piezoelectric resonators from $\text{La}_3\text{Ga}_5\text{SiO}_{14}$ (langasite) single crystals. *Proc. IEEE Frequency Control Symp.* 1992: 707–712. <https://doi.org/10.1109/FREQ.1992.269966>
8. Buzanov O.A., Zabelina E.V., Kozlova N.S. Optical properties of lanthanum-gallium tantalate at different growth and post-growth treatment conditions. *Crystallogr. Rep.* 2007; 52(4): 691–696. <https://doi.org/10.1134/S1063774507040177>
9. Uda S., Buzanov O. Growth of a 3" langasite crystal with clear faceting. *J. Cryst. Growth.* 2000; 211(1–4): 318–324. [https://doi.org/10.1016/S0022-0248\(99\)00788-5](https://doi.org/10.1016/S0022-0248(99)00788-5)
10. Kawanaka H., Takeda H., Shimamura K., Fukuda T. Growth and characterization of $\text{La}_3\text{Ta}_5\text{Ga}_5\text{O}_{14}$ single crystals. *J. Cryst. Growth.* 1998; 183(1–2): 274–277. [https://doi.org/10.1016/S0022-0248\(97\)00481-8](https://doi.org/10.1016/S0022-0248(97)00481-8)

11. Domoroshchina E.N., Dubovskii A.B., Kuz'micheva G.M., Semenkovich G.V. Influence of point defects on the electrical conductivity and dielectric properties of langasite. *Inorganic Materials*. 2005; 41(11): 1218–1221. <https://doi.org/10.1007/s10789-005-0290-y>
12. Zabelina E.V. *Neodnorodnosti v kristallakh lantan-gallievogo tantalata i ikh vliyaniye na opticheskie svoystva* [Inhomogeneities in crystals of lanthanum-gallium tantalate and their effect on optical properties]. Dis. of Cand. Sci. (Phys.-Math.). Moscow, 2018. 150 p. (In Russ.)
13. Kozlova N., Buzanov O., Zabelina E., Kozlova A., Voronova M., Shcherbachev K., Skryleva E. Study of the origin of the defects in $\text{La}_3\text{Ta}_{0.5}\text{Ga}_{3.5}\text{O}_{14}$ single crystals. *Optical Materials*. 2019; 91: 482–487. <https://doi.org/10.1016/j.optmat.2019.03.037>
14. Blistvan A.A., Geraskin V.V., Kozlova N.S. Influence of surface states on the features of phase transformations and the formation of structural defects in lithium iodate crystals. *Izvestiya vuzov. Tsvetnaya metallurgiya*. 1996; (4): 66–71. (In Russ.)
15. Blistanov A.A., Kozlova N.S., Geraskin V.V. The phenomenon of electrochemical self decomposition in polar dielectrics. *Ferroelectrics*. 1997; 198(1): 61–66. <https://doi.org/10.1080/00150199708228338>
16. Kozlova N.S., Zabelina E.V., Bykova M.B., Kozlova A.P. Features of manifestation of surface electrochemical processes in ferroelectric crystals with low-temperature phase transitions. *Izvestiya vuzov. Materialy elektronnoi tekhniki = Materials of Electronics Engineering*. 2018; 21(3): 146–155. (In Russ.). <https://doi.org/10.17073/1609-3577-2018-3-146-155>
17. Kozlova N.S., Zabelina E.V., Kozlova A.P. Features of behavior of near-electrode processes of dielectric crystals // 2019 IEEE International Symposium on Application of Ferroelectrics (ISAF).
18. Buzanov O.A., Zabelina E.V., Kozlova N.S., Sagalova T.B. Near-electrode processes in lanthanum-gallium tantalate crystals. *Crystallogr. Rep.* 2008; 53(5): 853–857. <https://doi.org/10.1134/S1063774508050210>
19. Buzanov O.A., Kozlova N.S., Zabelina E.V., Kozlova A.P., Siminel N.A. Effect of growth conditions on the optical transmission spectra and electrophysical properties of lanthanum-gallium silicate family crystals. *Izvestiya vuzov. Materialy elektronnoi tekhniki = Materials of Electronics Engineering*. 2010; (1): 14–19. (In Russ.)
20. Kong H.K., Wang J.Y., Zhang H.J., Yin X., Cheng X.F., Lin Y.T., Hu X B., Xu X.G., Jiang M.H. Growth and characterization of $\text{La}_3\text{Ga}_{3.5}\text{Ta}_{0.5}\text{O}_{14}$ crystal. *Cryst. Res. and Techn.* 2004; 39(8): 686–691. <https://doi.org/10.1002/crat.200310239>
21. Davulis P.M.; da Cunha M.P. A full set of langatate high-temperature acoustic wave constants: elastic, piezoelectric, dielectric constants up to 900 °C. *IEEE Trans. Ultrason. Ferroelectr. Freq. Control*. 2013; 60(4): 824–833. <https://doi.org/10.1109/TUFFC.2013.2631>
22. Zhukovskii V.M., Bushkova O.V. *Impedansnaya spektroskopiya tverdykh elektroliticheskikh materialov* [Impedance spectroscopy of solid electrolytic materials]. Yekaterinburg, 2000. 35 p. (In Russ.)
23. Frumkin A.N., Melik-Gaikazyan V.I. Determination of the kinetics of adsorption of organic substances by measuring the capacitance and conductivity of the electrode – solution interface. *Doklad AN SSSR*. 1951; 77(5): 855–858. (In Russ.)
24. Grafov B.M., Ukshe E.A. *Elektrokhimicheskie tsepi peremennogo toka* [Electrochemical alternating current circuit]. Moscow: Nauka, 1973. 128 p. (In Russ.)
25. *Kinetika slozhnykh elektrokhimicheskikh reaktsii* [Kinetics of complex electrochemical reactions]. Moscow: Nauka, 1981. 312 p. (In Russ.)
26. Yaokawa R., Uda S., Kimura H., Aota K. Electrical conduction mechanism in nonstoichiometric $\text{La}_3\text{Ta}_{0.5}\text{Ga}_{3.5}\text{O}_{14}$. *J. Appl. Phys.* 2010; 108(6): 064112-1–064112-9. <https://doi.org/10.1063/1.3478772>
27. Bjørheim T.S., Shanmugappirabu V., Haugrud R., Norby T.E. Protons in piezoelectric langatate: $\text{La}_3\text{Ta}_{0.5}\text{Ga}_{3.5}\text{O}_{14}$. *Solid State Ionics*. 2015; 278: 275–280. <https://doi.org/10.1016/j.ssi.2015.06.024>